

Contribution to the pathogenesis and early diagnosis of glaucoma. A Review

Lešták Ján^{1,2}, Pitrová Šárka¹, Aufrata Rudolf²,
Bednařík Milan¹

¹Faculty of Biomedical Engineering, Czech Technical University in Prague, Kladno, Czech Republic

²Department of Pediatric Ophthalmology, Faculty of Medicine, Masaryk University and University Hospital, Brno, Czech Republic

Submitted to the editorial board: January 13, 2026

Accepted for publication: April 23, 2026

Available on-line: June 1, 2026

The authors of the study declare that no conflict of interests exists in the compilation, subject and subsequent publication of this professional communication, and that it is not supported by any pharmaceuticals company. This study has not been submitted to any other journal or printed elsewhere, with the exception of congress abstracts and recommended procedures.



Doc. MUDr. Ján Lešták, CSc.

Correspondence address:

Fakulta biomedicínského inženýrství,

ČVUT v Praze

Náměstí Sítná 3105

272 01 Kladno

Czech Republic

E-mail: lestak@seznam.cz

SUMMARY

The aim of the work is to summarize recent observations on the pathogenesis of glaucoma, both from animal experiments and from clinical examinations of humans suffering from pathological intraocular pressure (IOP). Based on the knowledge gained, to present modern examination methods for diagnosing individual changes in the retinal vasculature and optic nerve papilla, the nerve fiber layer and retinal ganglion cells.

Conclusion: The highest statistical significance in the vasculature of the peripapillary and papillary areas was recorded in pathological IOP in the vessels inside the optic nerve disc. In the retinal nerve fiber layer (RNFL) after cleaning from vessel density, pathological values were recorded in vertical segments, i.e. in places where the axons of the retinal magnocellular ganglion cells enter the papilla. In the retinal ganglion cells, pathological changes were recorded when examining the far nasal part of the visual field.

Key words: glaucoma, pathogenesis, vessel density, retinal nerve fiber layer, changes in visual fields, early diagnosis

Čes. a slov. Oftal., 82, 2026, No. x, p.

INTRODUCTION

Glaucoma is the most common cause of irreversible blindness worldwide. The prevalence of this disease in the population aged over 40 years is approximately 3–5%, and according to estimates it is suffered by 60 million people [1,2]. The overall incidence within the population is within the range of 2–2.1% [3,4]. Taking into account the increasing number and proportion of aging persons within the population, it is expected that in 2040 glaucoma will affect 111.8 million people [5].

DEFINITION OF GLAUCOMA

Glaucoma is defined as an optic neuropathy that is characterized by changes on the papilla of the optic nerve (ON) and in the visual fields [6].

However, this definition is incomplete and requires correction. In the case of hypertensive glaucoma, primary damage to the retinal ganglion cells (RGCs) occurs, with subsequent damage to the entire visual pathway including the visual cortex of the brain [7]. It is important to keep in mind that glaucoma is characterized as a progressive pathology, in which an absolutely fundamental role for the preservati-

on of visual functions is played by timely determination of the diagnosis and commencement of adequate treatment.

With reference to the asymptomatic nature of the disease, its timely detection before the severe stages are manifested is difficult, and as a consequence the number of patients diagnosed with glaucoma is smaller than the number of undiagnosed [8,9]. For example, in China the rate of diagnosis of primary open-angle glaucoma is only 10% [10].

The above highlights the very important fact that the total number of patients affected by glaucoma may be far higher than the number represented in the statistics. Consequently, substantial emphasis is placed today on the timely diagnosis of this disease.

VASCULAR CHANGES AND THEIR TIMELY DIAGNOSIS

The retinal vasculature is a three-layered network composed of the superficial capillary plexus (SCP), the intermediate capillary plexus (ICP), and the deep capillary plexus (DCP). The SCP supplies nutrients to the retinal nerve fiber layer (RNFL), the retinal ganglion cells (RGCs) and the dendrites of the ON-RGCs in the inner plexiform layer (IPL). The ICP supplies nutrients to the OFF-RGCs in the

IPL and the amacrine cells in the inner nuclear layer (INL). The DCP supplies nutrients to the bipolar cells and the horizontal cells in the outer plexiform layer [11,12].

The prelaminar region of the ON papilla is supplied by the peripapillary choroid, composed of the posterior ciliary arteries and the recurrent choroidal arteries. The lamina cribiformis is supplied by the centripetal branches from the same arteries, either directly or through the formation of circles of Zinn-Haller. The retrolaminar region has peripheral centripetal vascular supply from the pial vascular network, and sometimes axial centrifugal supply from the central retinal artery [13].

The central retinal artery supplies blood to two thirds of the retina and the superficial nerve layer of the ON, although it provides only little or no vascular supply to the prelaminar, laminar and retrolaminar layers [14–16]. The short posterior ciliary arteries, which supply blood to the choroid and prelaminar part of the ON, form a connection with the capillary layers of the retina [17].

On a mouse model of glaucoma induced by unilateral cauterization of three episcleral veins it was observed that increased intraocular pressure (IOP) leads to disruption of autoregulation and vascular dysfunction of the retinal arterioles. This means that the capacity of the retinal arterioles to regulate blood flow and maintain correct vascular function was impaired [18,19]. Vascular dysfunction of the retina was observed as a secondary manifestation both in individuals with glaucoma and in animal models of this pathology, which indicates that glaucoma may also serve as a trigger of retinal vascular abnormalities [18].

Reduction of the number of capillaries in the retina observed in glaucoma-affected eyes in rats has a similar course, with a more pronounced impact on the density of the capillaries in the inner retinal layers in reaction to increased IOP. The three vascular capillary layers reacted differently to an increase of IOP. At IOP between 40 and 60 mmHg the capillaries of the DCP and ICP were markedly more resistant to the increase of IOP than the capillaries in the SCP. At an increase of IOP above 70 mmHg all layers of the retina manifested reduced vascular density. Change of vascular density in the SCP triggered by IOP was closely linked to a reduction in the thickness of the inner layers of the retina (nerve fibers, ganglion cells and inner plexiform layers). This close relationship between reduction of thickness of tissue and vascular density was less evident in the ICP and DCP [20]. This is very important information, since by contrast with RGCs, we are capable of diagnosing vascular changes quickly.

Similar conclusions were reached also by Tao et al., who following a temporary increase of IOP in mice determined vascular remodeling of the retina, in which the number of capillary branches was reduced in the superficial and intermediate capillary plexus. The number of RGCs, the diameter of the central retinal arterioles and the deep branching of the capillary plexus were not affected. These previously underappreciated findings indicate that a temporary increase of IOP may cause undetected and potentially long-term pathology of the RGCs and the connected neovascular units [21].

Similar changes were also recorded by Pitale et al.,

who following a temporary increase in IOP for a period of 2 weeks in a similar experiment on mice determined a normal number of RGCs but a substantial reduction in the capillary connections per mm^2 in the intermediate retinal capillary plexus, which spared the other plexuses. Capillary connection density, blood vessel length vascular surface were significantly reduced, and the number of acellular capillaries increased dramatically [22].

A very interesting article was presented by Diaz et al., who following an increase of IOP in rats measured capillary density, capillary volume, capillary length per unit of volume, capillary surface area per unit of volume and capillary diameter in the prelaminar, laminar and postlaminar region and in the optic nerve. They recorded the most pronounced changes in the postlaminar region [23].

We also focused on the vascular issue with a number of different IOP values. The first study on this theme compared the relationship of IOP with vessel density (VD), the RNFL and the visual field. The cohort comprised 122 healthy eyes. It was divided into four sub-groups. The first group comprised 18 eyes with an IOP value of < 20 mmHg. The second group comprised 39 eyes with IOP values of 20–22 mmHg. The third group comprised 32 eyes with IOP values of 22–24 mmHg, and the final group comprised 33 eyes with IOP values of > 24 mmHg. The results of intraocular pressure were compared with VD and the RNFL with the aid of a Pearson correlation coefficient in order to assess the relationship between the selected parameters. Depending on the value of the correlation coefficient it is possible to differentiate the following: weak ($|r| < 0.3$), medium ($0.3 < |r| < 0.8$) and strong ($|r| > 0.8$) linear dependency (correlation). The value p represents the statistical significance of the test. If this value is lower than 0.05, the correlation can be considered statistically significant.

Vessel density was measured in the peripapillary region. WI—whole image (4.5x4.5 mm) and PP (with diameter 3 mm). Figure 1. VD_a = vessel density of all blood vessels. VD_s = vessel density of small blood vessels. No correlation was found in eyes with normal IOP.

In eyes with IOP within the range of > 20 to ≤ 22 mmHg there was a statistically significant medium correlation with PP- VD_a ($r = -0.43$), PP- VD_s ($r = -0.45$), WI- VD_a ($r = -0.34$), WI- VD_s ($r = -0.48$) and RNFL ($r = -0.42$).

In eyes with IOP within the range of > 22 to ≤ 24 mmHg there was a statistically significant medium correlation with PP- VD_a ($r = -0.48$), PP- VD_s ($r = -0.53$), WI- VD_a ($r = -0.37$), WI- VD_s ($r = -0.54$) and RNFL ($r = -0.54$).

In eyes with IOP of > 24 mmHg there was a statistically significant medium correlation with PP- VD_a ($r = -0.56$), PP- VD_s ($r = -0.56$), WI- VD_a ($r = -0.53$), WI- VD_s ($r = -0.57$) and RNFL ($r = -0.59$) [24].

In another study we divided these overall VD values into individual peripapillary segments. Figure 2. The observed cohort comprised 104 eyes, of 26 women with an average age of 45 years and 26 men with an average age of 43 years. We observed the highest correlation with increasing IOP and VD in blood vessels (VD_a) of the whole image WI- VD_a ($r = -0.48$) and peripapillary vessels PP- VD_a ($r = -0.43$) and PP- VD_s ($r = -0.45$). When we evaluated the individual peripapillary

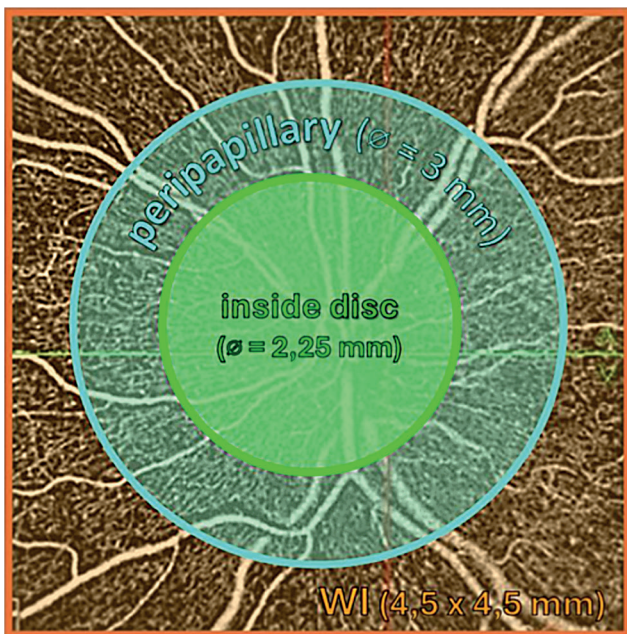


Figure 1. Areas of measured vessel density
 RNFL – retinal nerve fiber layer, WI – whole image, PP – peripapillary, ID – inside the disc

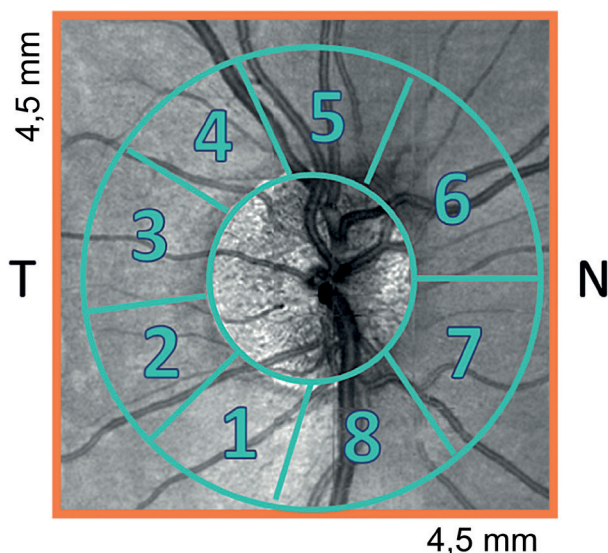


Figure 2. Labeling of individual peripapillary segments in which RNFL and VD thickness were assessed [25].
 RNFL – retinal nerve fiber layer, VD – vessel density, Inferior Temporal – IT (1), Temporal Inferior – TI (2), Temporal Superior – TS (3), Superior Temporal – ST (4), Superior Nasal – SN (5), Nasal Superior – NS (6), Nasal Inferior – NI (7), Inferior Nasal – IN (8)

segments (1–8), the highest correlation with increasing IOP was recorded in the IT segment – inferotemporal ($r = -0.48$), i.e., in the segment into which fibers of the magnocellular ganglion cells project from the inferotemporal quadrant [25].

If we return to the study by Diaz et al., who demonstrated on a rat model that the capillaries of the postlamina and to a lesser extent the lamina cribiformis of the ON are most susceptible to an increase of IOP [23], then for timely detection of changes it would be most appropriate to

measure VD precisely in these regions of the ON. Optical coherence tomography angiography (OCTA) instruments do not enable examination of VD in the deeper layers of the anterior part of the ON. This was attempted by Yoshikawa et al., who examined whether OCTA with enhanced depth imaging (EDI) was capable of detecting vascular signals in a glaucomatous optic disc. They determined that VD of the disc measured with the aid of EDI was significantly higher than VD measured by the conventional method, both in the case of glaucoma and in the case of eyes without glaucoma. VD of the disc was also significantly lower in the case of glaucoma than in patients without glaucoma [26].

Following on from the experimental study conducted by Diaz et al. [23], we also compared IOP with VD in the peripapillary region and inside the optic disc. The cohort comprised 100 eyes of 22 women with an average age of 52 years (20–78) and 28 men with an average age of 55 years (20–75). Visual acuity was 1.0 (with possible correction within the range of +1.5 to -3.0 D), and the patients did not have any other ocular pathology). IOP was measured with the aid of an Ocular Response Analyzer (ORA-Reichert). The resulting value was the average of three measurements. In 18 eyes IOP was lower than 21 mmHg (16–21 mmHg), while the other eye had IOP higher than 21 mmHg. In the majority of eyes the value was within the range of 21 to 36 mmHg. VD was measured with the aid of the instrument OCT System AngioVue™ (RTVue-XR, Optovue) in the peripapillary region (PP), in the whole image (WI) and inside the disc (ID), both in the case of all blood vessels (VDa), and small blood vessels (VDs). All the above examinations were performed without the use of artificial mydriasis.

There was a statistically significant relationship of age to IOP, even though this correlation was weak ($r = 0.241$). Medium values of correlation were recorded in PP-VDa ($r = -0.378$) and PP-VDs ($r = -0.389$). Higher values were recorded in WI-VDa ($r = -0.43$) and WI-VDs ($r = -0.44$). The highest correlation was determined in ID-VDa ($r = 0.52$). A weak correlation was recorded in ID-VDs ($r = -0.17$) [27].

The above conclusions of the results of measurement are very important, since they point to a disorder of VD in the prelaminar part of the ON. Perfusion of the prelaminar part of the optic disc in eyes with glaucoma has also been examined by other authors, with a result of reduced perfusion in the measured area. All compared healthy eyes with glaucomatous eyes [28–31].

To conclude this section we may state that we recorded the statistically highest correlation precisely inside the ON disc for all blood vessels (ID-VDa).

RETINAL GANGLION CELLS AND THEIR TIMELY DIAGNOSIS

The magnocellular ganglion cells of the retina are termed alpha, M, Y, or parasol in the literature. The parvocellular cells are referred to as beta, P, X, or midget.

The first structural changes to be observed following an increase of intraocular pressure in an experiment on monkeys related to structural abnormalities associated with

a reduction of the dendritic field of ganglion cells. A reduction in the thickness of axons appeared later, in which changes to the size of the cell soma appeared simultaneously or a little later. A chronic increase of IOP led to a significant reduction of the average soma size of midget and parasol cells, but only the parasol (magnocellular) cells showed a significant reduction of the size of the dendritic field and diameter of the axon. A comparison of eyes with different degrees of damage to the ON based on the cup-to-disc ratio showed that the axons and dendritic fields of the parasol cells at a lower c/d (cup-to-disc) ratio were significantly smaller than in the midget (parvocellular) cells, which indicates greater damage precisely to the magnocellular cells [32]. Similarly, Naskar et al. also demonstrated in an experiment that changes on the level of the ganglion cells occur earlier than changes in their axons [33].

A quantitative analysis in a case of experimental glaucoma induced in cats demonstrated that RGC density (alpha and beta), body size, maximum dendritic field radius, total dendrite length and the number of dendrite branches were markedly reduced in glaucomatous eyes in comparison with normal eyes. The loss of cells and reduction of dendrites in alpha (magnocellular) type ganglion cells in the retina was more pronounced than in the case of beta (parvocellular) type cells. Cell density of all types of cells in the retina decreased monotonously over time upon an increase of IOP, and the loss of cells was more pronounced in the case of large cells than small cells [34].

The dendritic fields of parasol and midget ganglion cells are smaller in the nasal retina than in the temporal retina at the same distance from the fovea [35]. Because the number of ganglion cells in the periphery of the temporal retina is smaller, their dendritic tree must be larger in order to cover the retina than in the nasal periphery. This is also supported by the study conducted by Gurcio and Allen, who determined that in the peripheral nasal retina the density of RGCs at corresponding eccentricities exceeds the temporal retina by more than 300%; the superior half exceeds the inferior by 60% [36]. If we calculate this to the number of magnocellular ganglion cells, there should therefore be approximately 10 000 ganglion cells in the periphery of the inferotemporal quadrant, 16 000 in the periphery of the superotemporal quadrant, 30 000 in the peripheral of the inferior nasal quadrant and 48 000 in the periphery of the superior nasal quadrant.

It logically follows from the fact that the magnocellular cells located in the temporal half of the retina are larger and have greater stromal branching that they must also have a greater energy consumption. As a result, in the case of a disorder of blood supply to the retina, these cells suffer the most from insufficient nutrition. Following their collapse (shrinking of the dendritic tree and the cell's somata) [32], changes take place precisely within the peripheral nasal part of the visual field.

Approximately 11–17% of eyes with a diagnosis of glaucoma or suspected glaucoma and a normal central visual field manifest defects outside the central scope of 30° [37–42]. Similar conclusions were reached also by Ma et al., who in 18% of eyes with a normal central visual field demonstrated glaucoma defects in the periphery of the visual field [43]. However, of these only measurement of

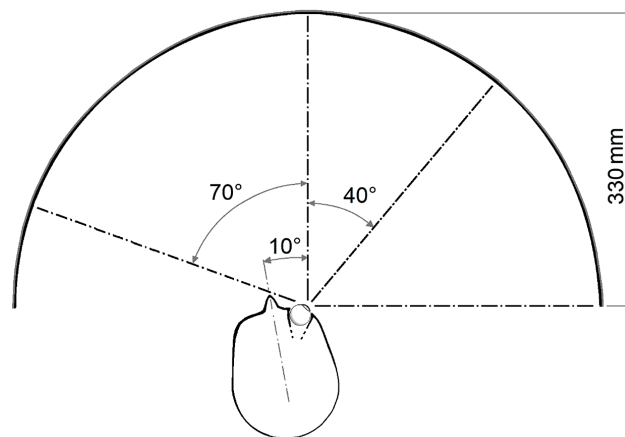


Figure 3. Head position and eye rotation 40° temporally [45]

the nasal periphery can provide us with sufficient information to supplement the information obtained through static testing in the central 30° in order to justify the additional time required for the examination [44].

For this reason we also attempted to examine this distal nasal part of the visual field. By shifting the fixation point 40° temporally we reached the nasal limit of the visual field at 100–110 degrees. Figure 3.

In all the examined eyes we determined the range of the nasally seen points at 100–110° (degrees) by perimetric examination. Of a total number of 30 eyes the limit of the nasal part was up to 100° in 13.3% of eyes, up to 105° in 20% of eyes, and up to 110° in up to 66.7% of eyes [45]. Figure 4.

When we performed the same examination on 60 eyes with primary open-angle glaucoma (POAG), we determined a depression of the distal periphery of the nasal part of the visual field within a range from 50 to 95°, in a normal visual field examined by a glaucoma program (22° temporally and 50° nasally) [46]. Figure 5.

In another study we demonstrated that changes did not occur in the overall values of the RNFL, even if abnormalities were diagnosed in the distal nasal part of the visual field. Upon a comparison of the results of the visual field with the RNFL values corrected by the VD in segment 5 (SN) we did not observe any correlation ($r = -0.03$), and only a very weak correlation in segment 8 ($r = -0.16$). We confirmed that alterations of the magnocellular ganglion cells localized in the temporal half of the retina anticipate changes in the RNFL. This applies not only in the overall values, but also in the values that are “adjusted” for VD in the segments where the axons of the magnocellular cells project into the ON disc. The introduction of examination of the distal nasal visual field in patients with suspected POAG and eyes with intraocular hypertension (IOH) may confirm the diagnosis earlier than previous methods. From our perspective this could have an impact not only in terms of health but also socially [47].

We demonstrated that this may indeed concern a collapse of the magnocellular ganglion cells of the retina in early POAG, in a study in which we observed the distal nasal part of the visual field in 50 eyes before and after treatment. One

month after commencing treatment with carteolol, we recorded an improvement of the average number of unseen points from 16.7 to 9.5 5 ($p = 0,006$) [48]. Figures 6–9.

In the conclusion of this chapter we may state that examination of the peripheral nasal part of the visual field in

early glaucoma provides better results than examination of the central part of the VF and RNFL. At the same time, we demonstrated that in the initial stages the “collapse” of the RGCs may be only a temporary manifestation if the cause is eliminated.

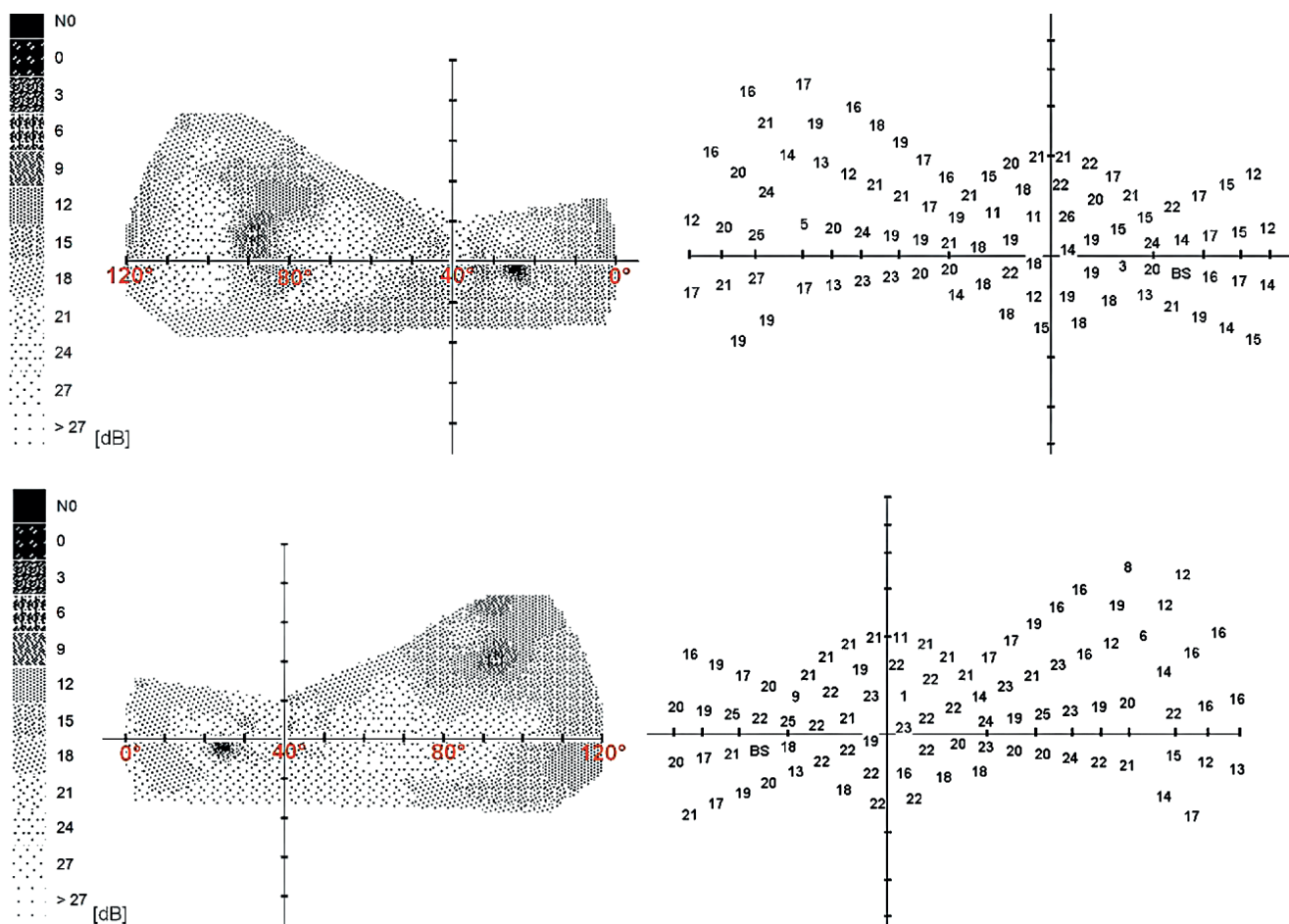


Figure 4. The extent of the nasal part of the visual field and the distribution of the examined points. Above – right eye, below – left eye [45]

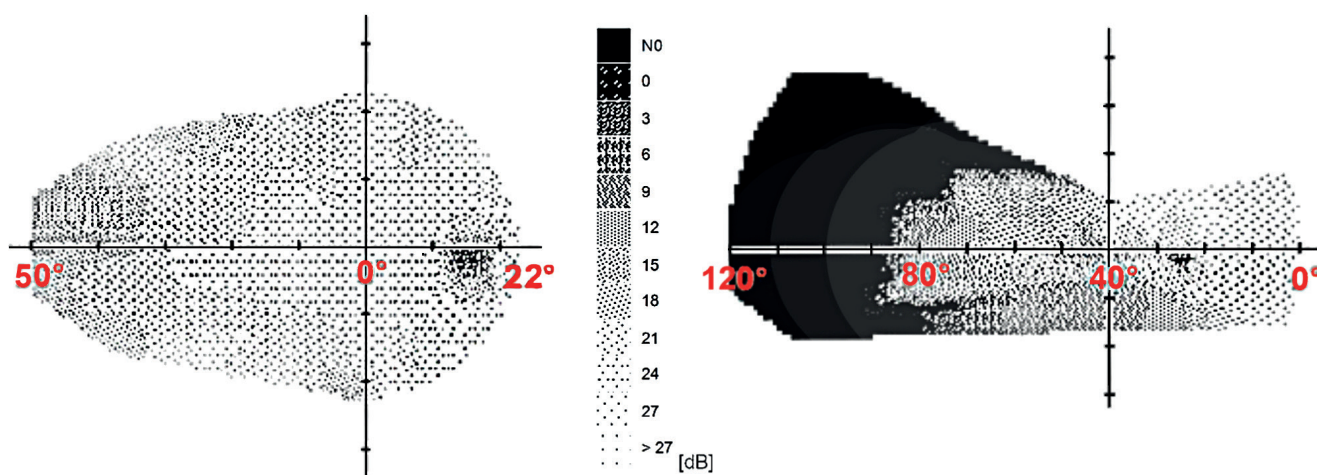


Figure 5. Difference in visual field changes in the right eye of a patient with glaucoma. On the left, a conventional glaucoma template with a fast threshold strategy with a range of 50° nasally and 22° temporally. On the right, nasal depression in the same eye using an extended template with a horizontal range of 120°. The fixation point is at 0° [46]

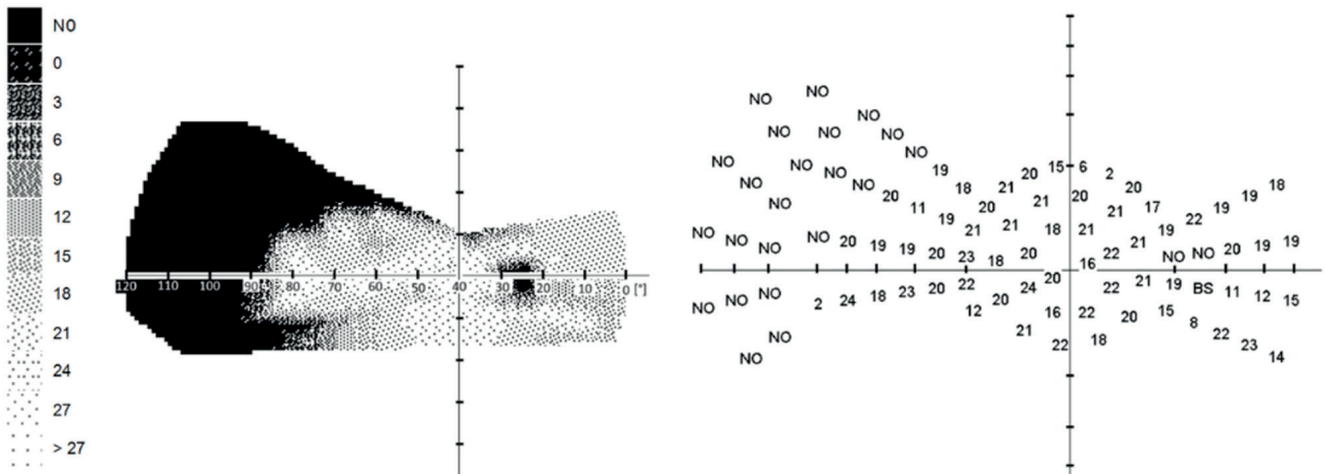


Figure 6. Nasal part of the right visual field before treatment with carteolol. Visual field in grayscale (left) and numerical values with unseen dots (right)

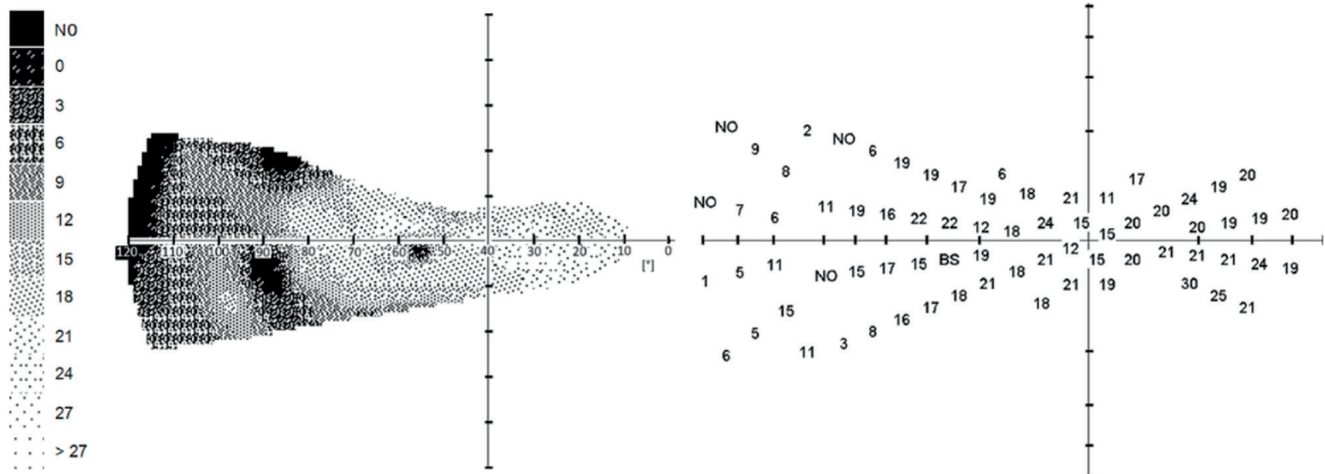


Figure 7. Nasal part of the right visual field before treatment with carteolol. Visual field in grayscale (left) and numerical values with unseen dots (right)

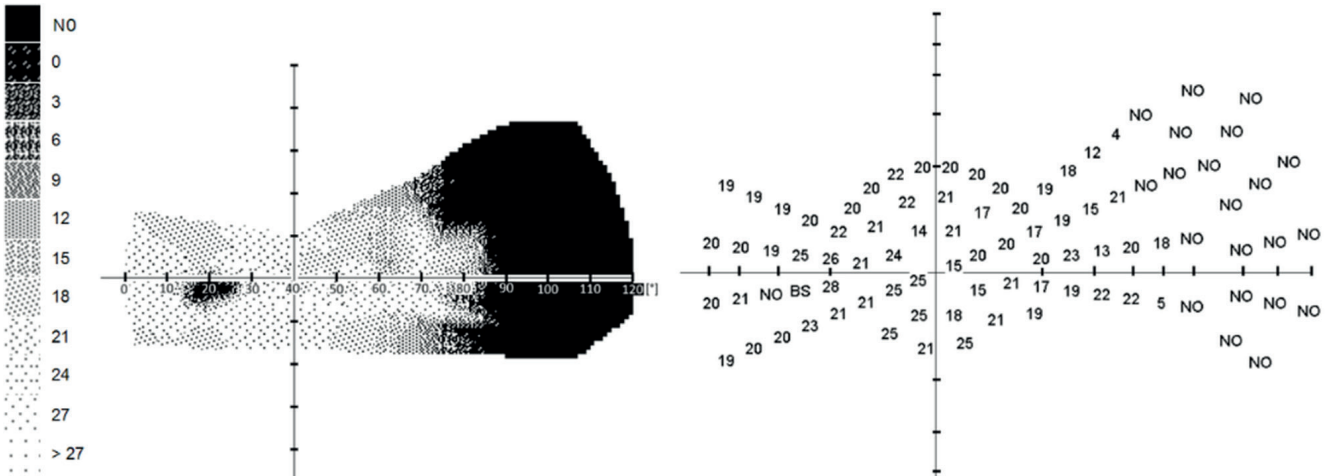


Figure 8. Nasal portion of left visual field before treatment with carteolol. Visual field in grayscale (left) and numerical values with unseen dots (right)

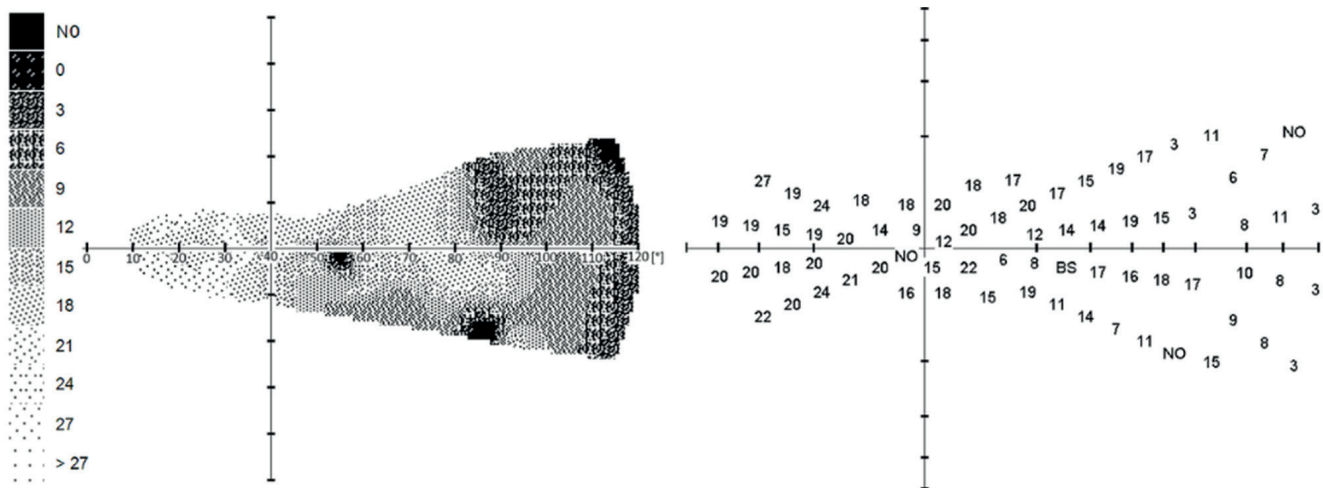


Figure 9. Nasal portion of left visual field after treatment with carteolol. From 21 blind spots, the finding improved to 3 blind spots. Visual field in grayscale (left) and numerical values with blind spots (right)

CHANGES IN THE RNFL AND THEIR TIMELY DIAGNOSIS

Disruption of the retinal axons was demonstrated as early as in 1976 by Vrabec in histological preparations in a localized narrow transverse strip on the level of the posterior lamina cribrosa and immediately beyond it. The retinal axons in front of this zone were mostly intact [49]. This was also verified in an experiment by Soto et al., who using a mouse model determined that degeneration of RGCs in glaucoma has two separate stages: the first covers atrophy of the ganglion cells and the second damage to their axons. Retrolaminar degeneration of the axons takes place before the degeneration of their intraretinal part [50]. Further studies by Quigley et al. also demonstrated significant thinning of the RNFL in the inferior quadrant in eyes with IOH in comparison with healthy eyes. The finding that incipient thinning of the RNFL takes place in the inferior quadrant of eyes with intraocular hypertension is especially interesting. Defects of the ON associated with glaucoma often occur initially on the inferior pole [51,52].

The fact that this predominantly concerns fibers of the magnocellular cells was also confirmed by a study conducted by Quigley et al. Fibers with a larger diameter withered more rapidly than smaller fibers, although no size of fibers was completely spared in any stage of atrophy [53]. A computer analysis of the image was used to determine the normal number of axons and the distribution of the diameter of axons in 12 normal human eyes. The average number of axons per nerve was $969\,279 \pm 239\,740$ and the average diameter of the axons was $0.72 \pm 0.07 \mu\text{m}$. Multiple linear regression detected 4 909 axons lost per year ($p = 0.08$) [54]. Despite the fact that retinal magnocellular cells wither earlier in hypertensive glaucoma than their axons, their diagnosis is complex.

It is evident that in the early stages of hypertensive glaucoma, when the first changes in the RGCs take place, we cannot even theoretically determine a reduction of sensitivity in the central part of the visual field [55]. As a con-

sequence, it is more appropriate and accessible to examine their axons on the ON disc, where their concentration is highest. With reference to the fact that their average values are used in evaluating the RNFL, we were interested in whether their loss would be more pronounced in certain segments. This would be of fundamental importance for timely diagnosis and subsequent timely treatment.

In the study, in which we observed the influence of IOP on the RNFL and VD, we did not determine any correlation between IOP and the RNFL in eyes with normal IOP ($r = -0.06$). In eyes with IOP of NOT 20–22 mmHg there was a medium correlation ($r = -0.42$). A similar situation applied also in eyes with IOP of 22–24 mmHg ($r = -0.48$) and in eyes with IOP of 24 mmHg and higher ($r = -0.59$) [56].

In another study which examined the relationship between pathological intraocular pressure and the RNFL in the individual peripapillary segments, the highest correlation was determined in segments 1, 4, 5 and 8. Here axons of predominantly damaged magnocellular ganglion cells project into the ON papilla [57].

Because the blood vessels also contribute to the thickness of the RNFL to a considerable degree, for the sake of determining this thickness accurately we decided to “adjust” the RNFL for VD.

Hood et al. demonstrated that VD plays a significant role in RNFL thickness and that ~13% of the total thickness of the peripapillary RNFL in healthy individuals is attributed to the blood vessels [58]. Similarly, Patel et al. detected that blood vessels constitute 9.3% of the total thickness or surface of the RNFL, but differ according to their location on the retina. On average 17.6% of the superior and 14.2% of the superior RNFL is formed by blood vessels, whereas blood vessels constitute only 2.3% of the surface of the temporal and nasal RNFL [59]. Pereira et al. state that according to their model, circumpapillary distribution of the retinal blood vessels is influenced by VD up to 70% of the thickness of the RNFL [60]. Allegrini et al. further determined that the vascular proportion of

RNFL thickness constitutes $29.07 \pm 3.95\%$ [61].

In our own published study we recorded the largest influence of pathological IOP on VD in segments 1, 4, 5, 6, 7 and 8, and on the RNFL in segments 1, 4, 5 and 8. After "adjustment" of RNFL thickness for VD, the highest correlation in this study was observed in segments 5 ($r = -0.32$, $p = 0.002$) and 8 ($r = -0.39$, $p = 0.001$), i.e. in the locations where the thickest axons of ganglion cells, corresponding to the magnocellular cells, project into the optic disc. The other segments were statistically insignificant. Consequently, in the early stages of hypertensive glaucoma this study recommends evaluation of the RNFL in the superior and inferior segments of the peripapillary region of the ON.

In conclusion we may state that his study detected the most significant damage to the RNFL in the inferior and superior segments after "adjustment" for VD, which is the place where the magnocellular fibers are located [62]. This is also in accordance with the histological findings.

An analysis conducted by Drenhaus et al. detected different groups of axon diameters, with the following average diameters of axons and proportions. The group of small axons with a diameter of 0.55 micrometers constituted 70%. The group of medium-sized axons with a diameter of 1.39 microns formed 10% [63]. A post-mortem examination showed that the most susceptible fibers of the ON papilla are evidently located within a zone in the shape of an hourglass, in which the two widest sections are situated at 12 and 6 o'clock [64,65]. Tu et al. determined that the most sensitive quadrants to an increase of IOP in monkeys are the inferior and superior quadrants, in which the speed of changes in the RNFL is virtually parallel to the level of IOP [66]. Similar conclusions were drawn by Bowd et al. in relation to humans. The average RNFL value was significantly thinner in ocular hypertension than in normal eyes, specifically $72.8 \mu\text{m}$ ($66.4\text{--}78.1 \mu\text{m}$), and $85.8 \mu\text{m}$ ($80.2\text{--}91.7 \mu\text{m}$) respectively. More precisely speaking, the RNFL was significantly thinner in ocular hypertension than in normal eyes in the inferior quadrant. In

their publication, Bowd et al. state that the basis of these observations is unknown. It is possible that thinning of the RNFL in the inferior quadrant of eyes with IOH is an early form of glaucoma, which precedes detectable disorders of the ON and/or visual field. Another possibility is that the RNFL in eyes with IOH may be thin to begin with in the inferior quadrant, which makes these eyes particularly susceptible to the effects of increased IOP [67].

It is evident from the study conducted by Gurcio that the density of RGCs in the periphery of the human retina is lowest in the inferior temporal quadrant, followed by the superior temporal quadrant [36]. This is also reflected in the projections into the ON disc in the inferior temporal and superior temporal sector. If the magnocellular cells located in the inferior temporal quadrant of the retina suffer most from insufficient nutrition in the case of high IOP, their loss on the ON disc is most evident also with reference to the thickness of their axons. If the same number of parvocellular and magnocellular RGCs wither, the loss of RGCs on the ON disc is more evident as a result of the thickness of their axons (1.39 , vs. $0.55 \mu\text{m}$).

To conclude this section we may state that an increase of IOP contributes more significantly to VD than corrected RNFL. Damaged RGC fibers can be best determined on the ON papilla in vertical segments.

CONCLUSION

The highest statistical significance in the vasculature of the peripapillary and papillary region was recorded in pathological IOP in the blood vessels inside the ON disc. Following adjustment for vessel density, in the retinal nerve fiber layer pathological values were recorded in the vertical segments, i.e., in locations where the axons of the retinal magnocellular cells project into the disc. Pathological changes were recorded in retinal ganglion cells upon an examination of the distal nasal part of the visual field.

REFERENCES

1. Jonas JB, Aung T, Bourne RR, et al. Glaucoma. *Lancet*. 2017;390:2183-2193.
2. Quigley HA, Broman AT. The number of people with glaucoma worldwide in 2010 and 2020. *Br J Ophthalmol*. 2006;90:262-267.
3. Klein BE, Klein R, Sponsel WE. Prevalence of glaucoma. The Beaver Dam Eye Study *Ophthalmology* 1992; 99:1499-1504.
4. Bonomi L, Marchini G, Marraffa M. Prevalence of glaucoma and intraocular pressure distribution in a defined population. The Egna-Neumarkt Study *Ophthalmology*. 1998; 105:209-215.
5. Tham YC, Li X., Wong TY, Quigley HA, Aung T, Cheng CY. Global prevalence of glaucoma and projections of glaucoma burden through 2040: a systematic review and meta-analysis. *Ophthalmology*. 2014;121:2081-2090.
6. Quigley HA. 21st century glaucoma care. *Eye (Lond)*. 2019;33:254-260. doi: 10.1038/s41433-018-0227-8
7. Lestak J, Fus M. Neuroprotection in glaucoma – a review of electrophysiologist. *Exp Ther Med*. 2020;19:2401-2405.
8. Burgoyne CF, Downs JC, Bellezza AJ, Suh JK, Hart RT. The optic nerve head as a biomechanical structure: a new paradigm for understanding the role of IOP-related stress and strain in the pathophysiology of glaucomatous optic nerve head damage. *Prog Retin Eye Res*. 2005;24:39-73.
9. Weinreb RN, Aung T, Medeiros FA. The pathophysiology and treatment of glaucoma: a review. *Jama*. 2014;311:1901-1911.
10. Gedde SJ, Vinod K, Wright MM, et al. Primary Open-Angle Glaucoma Preferred Practice Pattern. *Ophthalmology*. 2021;128:71-150.
11. Usui Y, Westenskow PD, Kurihara T, et al. Neurovascular crosstalk between interneurons and capillaries is required for vision. *J Clin Invest*. 2015;125: 2335-2346. doi: 10.1172/JCI80297
12. Nian S, Lo A C Y, Mi Y, Ren K, Yang D. Neurovascular unit in diabetic retinopathy: pathophysiological roles and potential therapeutic targets. *Eye Vis. (Lond)* 2021;8:15. doi: 10.1186/s40662-021-00239-1
13. Hayreh S.S. The blood supply of the optic nerve head and the evaluation of t- myth and reality. *Prog Retin Eye Res*. 2001;20:563-593.
14. Hayreh, SS. Blood supply of the optic nerve head and its role in optic atrophy, glaucoma and oedema of the optic disc. *Br J Ophthalmol*. 1969;53:721-748.
15. Hayreh SS. Anterior ischemic optic neuropathy. *Clin Neurosci*. 1997;4:251-463.
16. Mackenzie PJ, Cioffi GA. Vascular anatomy of the optic nerve head. *Can J Ophthalmol*. 2008;43:308-312.
17. McAllister AS. A Review of the Vascular Anatomy of the Optic Nerve Head and Its Clinical Implications. *Cureus*. 2013;5:e98. DOI 10.7759/cureus.98

18. Gericke A, Mann C, Zadeh JK et al. Elevated Intraocular Pressure Causes Abnormal Reactivity of Mouse Retinal Arterioles. *Oxid Med Cell Longev*. 2019;9736047. doi: 10.1155/2019/9736047
19. Ruiz-Ederra J, Verkman AS. Mouse model of sustained elevation in intraocular pressure produced by episcleral vein. *Exp Eye Res*. 2006;82:879-884.
20. Zhao D, He Z, Wang L, Fortune B, Lim JK. Response of the Trilaminar Retinal Vessel Network to Intraocular Pressure Elevation in Rat Eyes. *Invest Ophthalmol Vis Sci*. 2020;61:2. doi: 10.1167/iovs.61.2.2
21. Tao X, Sigireddi RR, Westenskow PD, Channa R, Frankfort BJ. Single transient intraocular pressure elevations cause prolonged retinal ganglion cell dysfunction and retinal capillary abnormalities in mice. *Exp Eye Res*. 2020;201:108296. doi: 10.1016/j.exer.2020.108296
22. Pitale PM, Shen G, Sigireddi RR, et al. Selective vulnerability of the intermediate retinal capillary plexus precedes retinal ganglion cell loss in ocular hypertension. *Front Cell Neurosci*. 2022;16:1073786. doi: 10.3389/fncel.2022.1073786
23. Diaz F, Villena A, Vidal L, Moreno M, García-Campos J, Pérez de Vargas I. Experimental model of ocular hypertension in the rat: study of the optic nerve capillaries and action of hypotensive drugs. *Invest Ophthalmol Vis Sci* 2010;51:946-955.
24. Kral J, Lestak J, Nutterova E. OCT angiography, RNFL and the visual field at different values of intraocular pressure. *Biomed Rep*. 2022;16:36. doi: 10.3892/br.2022.1519
25. Král J, Lešták J, Füs M. Cévní hustota a tloušťka vrstvy nervových vláken u patologického nitroočního tlaku. *Cesk Slov Oftalmol*. 2025;81:182-186.
26. Yoshikawa Y, Shoji T, Kanno J, Kimura I, Hangai M, Shinoda K. Optic disc vessel density in nonglaucomatous and glaucomatous eyes: an enhanced-depth imaging optical coherence tomography angiography study. *Clin Ophthalmol*. 2018;19:12:1113-1119. doi: 10.2147/OPTH.S16722
27. Lešták J, Pochop P, Mikšovský J. Vessel density in the peripapillary and papillary areas at different intraocular pressure values. *Medicine*, in press.
28. Bojikian KD, Chen CL, Wen JC, et al. Optic Disc Perfusion in Primary Open Angle and Normal Tension Glaucoma Eyes Using Optical Coherence Tomography-Based Microangiography. *PLoS One*. 2016;11(5):e0154691. doi: 10.1371/journal.pone.0154691
29. Chen CL, Bojikian KD, Gupta D, et al. Optic nerve head perfusion in normal eyes and eyes with glaucoma using optical coherence tomography-based microangiography. *Quant Imaging Med Surg*. 2016;6:125-133. doi: 10.21037/qims.2016.03.05
30. Numa S, Akagi T, Uji A, et al. Visualization of the Lamina Cribrosa Microvasculature in Normal and Glaucomatous Eyes: A Swept-source Optical Coherence Tomography Angiography Study. *J Glaucoma*. 2018;27:1032-1035. doi: 10.1097/IJG.0000000000001069
31. Nascimento E, Silva R, Chiou CA, et al. Microvasculature of the Optic Nerve Head and Peripapillary Region in Patients With Primary Open-Angle Glaucoma. *J Glaucoma*. 2019;28:281-288. doi: 10.1097/IJG.0000000000001165
32. Weber AJ, Kaufman PL, Hubbard WC. Morphology of single ganglion cells in the glaucomatous primate retina. *Invest Ophthalmol Vis Sci*. 1998;39:2304-2320.
33. Naskar R, Wissing M, Thanos S. Detection of Early Neuron Degeneration and Accompanying Microglial Responses in the Retina of a Rat Model of Glaucoma. *Invest Ophthalmol Vis Sci*. 2002;43:2962-2968.
34. Shou T, Liu J, Wang W, Zhou Y, Zhao K. Differential dendritic shrinkage of alpha and beta retinal ganglion cells in cats with chronic glaucoma. *Invest Ophthalmol Vis Sci*. 2003;44:3005-3010.
35. Perry VH, Oehler R, Cowey A. Retinal ganglion cells that project to the dorsal lateral geniculate nucleus in the macaque monkey. *Neuroscience*. 1984;12:1101-1123. doi: 10.1016/0306-4522(84)90006-x
36. Gurcio CA, Allen KA. Topography of ganglion cells in human retina. *J Comp Neurol*. 1990;300:5-25.
37. Caprioli J, Spaeth GL. Static threshold examination of the peripheral nasal visual field in glaucoma. *Arch Ophthalmol*. 1985;103:1150-1154.
38. Seamone C, LeBlanc R, Rubilowicz M, Mann C, Orr A. The value of indices in the central and peripheral visual fields for the detection of glaucoma. *Am J Ophthalmol*. 1988;106:180-185.
39. Miller KN, Shields MB, Ollie AR. Automated kinetic perimetry with two peripheral isopters in glaucoma. *Arch Ophthalmol*. 1989;107:1316-1320.
40. Ballon BJ, Echelman DA, Shields MB, Ollie AR. Peripheral visual field testing in glaucoma by automated kinetic perimetry with the Humphrey field analyzer. *Arch Ophthalmol*. 1992;110:1730-1732.
41. LeBlanc EP, Becker B. Peripheral nasal field defects. *Am J Ophthalmol*. 1971;72:415-419.
42. Odden JL, Mihailovic A, Boland MV, Friedman DS, West SK, Ramulu PY. Evaluation of Central and Peripheral Visual Field Concordance in Glaucoma. *Invest Ophthalmol Vis Sci*. 2016;57:2797-2804.
43. Ma X, Tang L, Chen X, Zeng L. Periphery kinetic perimetry: clinically feasible to complement central static perimetry. *BMC Ophthalmol*. 2021;23:21:343. doi:10.1186/s12886-021-02056-5
44. Stewart WC, Shields MB. The peripheral visual field in glaucoma: reevaluation in the age of automated perimetry. *Surv Ophthalmol*. 1991;36:59-69.
45. Lešták J, Füs M, Lešták T, Pitrová Š. The Far Nasal Part of the Visual Field - Part I. *Cesk Slov Oftalmol*. 2023;79:306-309.
46. Lešták J, Füs M, Lešták T, Pitrová Š. The Far Nasal Part of the Field of Vision - Part II. Contribution to the Timely Diagnosis of Glaucoma. *Cesk Slov Oftalmol*. 2023;79(6):312-316.
47. Lestak J, Fus M, Pitrova S. Distal Nasal Part of the Visual Field and RNFL in Primary Open-Angle Glaucoma. *Clin Ophthalmol*. 2024;18:1-7.
48. Lestak J, Autrata R, Miksovsky J, Bednarik M. Effects of Anti-Glaucoma Drugs on the Distal Nasal Visual Field, Retinal Nerve Fiber Layer, and Vessel Density in Preperimetric Primary Open-Angle Glaucoma. *Biomedicine*, in press.
49. Vrabec F. Glaucomatous cupping of the human optic disc: a neuro-histologic study. *Albrecht Von Graefes Arch Klin Exp Ophthalmol*. 1976;198:223-234.
50. Soto I, Oglesby E, Buckingham BP, et al. Retinal Ganglion Cells Downregulate Gene Expression and Lose Their Axons within the Optic Nerve Head in a Mouse Glaucoma Model. *J Neurosci*. 2008;28:548-561.
51. Quigley HA, Addicks EM, Green WR, Maumenee AE. Optic nerve damage in human glaucoma. II: the site of injury and susceptibility to damage. *Arch Ophthalmol*. 1981;99:635-649.
52. Quigley HA, Hohman RM, Addicks EM, Massof RW, Green WR. Morphological changes in the lamina cribrosa correlated with neural loss in open-angle glaucoma. *Am J Ophthalmol*. 1983;95:673-691.
53. Quigley HA, Dunkelberger GR, Green WR. Chronic human glaucoma causing selectively greater loss of large optic nerve fibers. *Ophthalmology*. 1988;95:357-363. doi: 10.1016/s0161-6420(88)33176-3
54. Mikelberg FS, Drance SM, Schulzer M, Yidegiligne HM, Weis MM. The normal human optic nerve. Axon count and axon diameter distribution. *Ophthalmology*. 1989;96:1325-1328.
55. Lešták J, Füs M. Visual field assessment in hypertension glaucoma. *Cesk Slov Oftalmol*. 2021;77:20-24.
56. Kral J, Lestak J, Nutterova E. OCT angiography, RNFL and visual field at different values of intraocular pressure. *Biomed Rep*. 2022;16:36. doi: 10.3892/br.2022.1519
57. Lešták J, Füs M, Král J. The Relationship Between the Thickness of RNFL in Segments and Intraocular Pressure. *Clin Ophthalmol*. 2022;16:3673-3679.
58. Hood DC, Fortune B, Arthur SN, et al. Blood vessel contributions to retinal nerve fiber layer thickness profiles measured with optical coherence tomography. *J Glaucoma*. 2008;17:519-528.
59. Patel N, Luo X, Wheat JL, Harwerth RS. Retinal nerve fiber layer assessment: Area versus thickness measurements from elliptical scans centered on the optic nerve. *Invest Ophthalmol Vis Sci*. 2011;52:2477-2489.
60. Pereira J, Weber S, Holzer S, et al. Correlation between retinal vessel density profile and circumpapillary RNFL thickness measured with Fourier-domain optical coherence tomography. *Br J Ophthalmol*. 2014;98:538-543.
61. Allegrini D, Montesano G, Fogagnolo P, et al. The volume of peripapillary vessels within the retinal nerve fibre layer: An optical coherence tomography angiography study of normal subjects. *Br J Ophthalmol*. 2018;102:611-621.
62. Lešták J, Füs M, Král J. Axons of retinal ganglion cells on the optic nerve disc following vessel density correction at different IOP values. *Exp Ther Med*. 2023;19:25:261. doi: 10.3892/etm.2023.11960
63. Drenhaus U, von Gunten A, Rager G. Classes of axons and their distribution in the optic nerve of the tree shrew (*Tupaia belangeri*) *Anat Rec*. 1997;249:103-116.
64. Quigley HA, Addicks EM. Regional differences in the structure of the lamina cribrosa and their relation to glaucomatous optic nerve damage. *Arch Ophthalmol*. 1981;99:137-143.
65. Quigley HA, Addicks EM, Green WR. Optic nerve damage in human glaucoma: 111. Quantitative correlation of nerve fiber loss and visual field defect in glaucoma, ischemic neuropathy, papilledema, and toxic neuropathy. *Arch Ophthalmol*. 1982;100:135-146.
66. Tu S, Li K, Ding X, Hu D, Li K, Ge J. Relationship between intraocular pressure and retinal nerve fibre thickness loss in a monkey model of chronic ocular hypertension. *Eye (Lond)*. 2019;33:1833-1841. doi: 10.1038/s41433-019-0484-1
67. Bowd C, Weinreb RN, Williams JM, Zangwill LM. The retinal nerve fiber layer thickness in ocular hypertensive, normal, and glaucomatous eyes with optical coherence tomography. *Arch Ophthalmol*. 2000;118:22-26. doi: 10.1001/archoph.118.1.22